Strojnícky časopis – *Journal of* MECHANICAL ENGINEERING,
VOL 76 (2026), NO 1, 7 – 16

A NEW APPROACH TO SUSPENSION CONTROL: PID COMBINED SKYHOOK

BİLGİÇ Boğaç[1*]

[1] *Department of Mechanical Engineering, Faculty of Engineering, Istanbul University – Cerrahpasa 34320 Istanbul, Türkiye, e-mail: bogac@iuc.edu.tr*

Abstract: This study introduces a control approach that enhances a PID-based active suspension with a skyhook-inspired semi-active effect. PID is widely used in active systems, while skyhook provides effective damping for semi-active setups. The method combines the PID force with an adaptive algorithm that mimics skyhook behaviour. This allows a single actuator to benefit from both control types. The resulting controller, PIDcSky (PID combined Skyhook), offers a simple way to bring semi-active advantages into active designs.

KEYWORDS: Skyhook, PID controller, suspension control, active control

1 Introduction

The PID controller, which can be successfully applied to many well-known systems, has been derived from various versions until today, and books have been written on it and explained in detail [1, 2]. Although it is an old method for tuning PID controllers, the Ziegler-Nichols Method, which is quite successful, is widely used [3]. The application of the PID controller, in which the coefficients found by this method are used, to vehicle suspensions is also encountered in reference books. Studies carried out close to today, it has been tried to find suitable coefficients for vehicle suspension systems by minimizing the objective function determined by various optimization techniques [4, 5]. In addition, studies were carried out in which the coefficients were changed adaptively by adding a fuzzy controller [6]. With these studies, the PID controller has been further improved and has become a cornerstone for active controllers. Therefore, the controllers recommended in many studies are given by comparing them with the PID controller.

Due to the high power consumption of active controllers, semi-active controllers are used in suspension systems. Mostly, control algorithms are designed based on physically changing the damping coefficient. Since they are not generally power generators, although they do not achieve as much success as active controllers, they have been a successful alternative as simple and low-power consumption controllers by nature. The Skyhook model has been adapted to vehicle suspension systems as a semi-active controller and has achieved very successful results [7]. In later studies, semi-active control algorithms were created by combining many mixed methods [8]. It is frequently used in algorithms imitating active controllers, as well as controlling semi-active elements directly with fuzzy controllers [9-10].

Despite all these studies, a single active controller that will create the effect of active and semi-active systems alone has not been designed in the literature. In this study, the most known active controller and semi-active controller methods were combined and only the active controller was provided to produce it. By combining the skyhook algorithm with the PID controller, a controller with successful features of both was obtained and named PIDcSky (PID

DOI: 10.2478/scjme-2026-0002, Print ISSN 0039-2472, On-line ISSN 2450-5471

combined skyhook). This study, which is done by choosing basic controllers, can be applied to other active and semi-active controllers with appropriate modifications. In future studies, if the same naming is used in the application, a common name will be provided for these newly produced control algorithms in terms of literature. For example, PIDcGround (PID combined Groundhook). These studies are excluded from this article so as not to miss the basic logic. Studies on these can be done in the future, and these controllers can be applied in different fields. In particular, it is readily adaptable to air spring systems that have previously been regulated using conventional PID or alternative control algorithms [11]. Furthermore, the proposed approach can be extended to more sophisticated seat suspension models as well as motorcycle dynamic models, demonstrating its robustness and applicability to complex mechanical systems [12-13].

Skyhook stands out as a highly effective control algorithm in the realm of semi-active controllers, while PID is a well-established algorithm in the domain of active controllers. Within systems employing an active controller, there exists the capability not only to generate its own control signal but also to emulate the signal produced by a semi-active controller. This emulation involves envisioning the integration of a semi-active controller within the system's dynamics. Through the synthesis of both control signals, the system can function as if it hosts both an active controller and a semi-active controller. This innovative strategy facilitates the utilization of advantageous features provided by the semi-active controller in conjunction with the attributes of an active controller.

2 Mathematical Model and Road Input

In general, suspension systems can be classified into three categories: passive, active, and semi-active. In this study, a new controller approach was designed and its effectiveness is demonstrated using the simplest linear quarter vehicle model. Fig. 1 provides a symbolic representation of these three types of suspension systems. Furthermore, the mathematical equations governing these systems differ due to their structural characteristics.

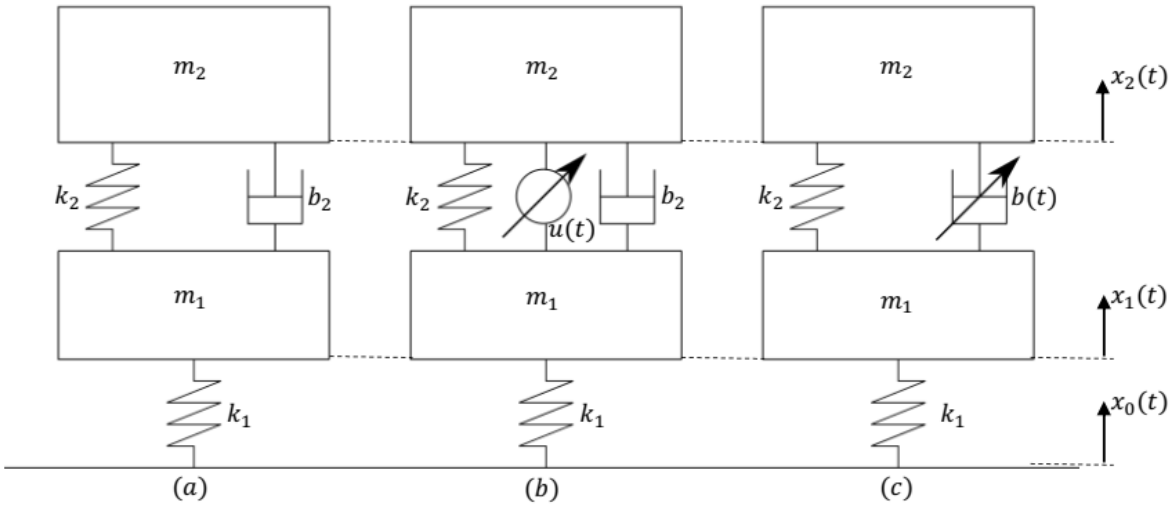

Fig. 1 (a) Passive (b) Active (c) Semi-active suspension model for quarter car

$$m_2\ddot{x}_2 + b_2(\dot{x}_2 - \dot{x}_1) + k_2(x_2 - x_1) = 0 \quad (1)$$

$$m_1\ddot{x}_1 + b_2(\dot{x}_1 - \dot{x}_2) + k_2(x_1 - x_2) + k_1(x_1 - x_0) = 0 \quad (2)$$

Eq. 1 and Eq. 2 are ordinary differential equations that describe the behaviour of the passive suspension system in response to the road input. In these equations, m_1 represents the mass of the wheel, and m_2 represents the quarter mass of the car body. Passive suspension systems are characterized by having constant coefficients in the equations that govern their behaviour. This means that the values of b_2 (damping coefficient of the suspension system), k_1 (coefficient of the wheel spring), and k_2 (coefficient of the suspension spring) do not change during operation and remain fixed values throughout the system's operation.

$$m_2\ddot{x}_2 + b_2(\dot{x}_2 - \dot{x}_1) + k_2(x_2 - x_1) = u \tag{3}$$

$$m_1\ddot{x}_1 + b_2(\dot{x}_1 - \dot{x}_2) + k_2(x_1 - x_2) + k_1(x_1 - x_0) = -u \tag{4}$$

Eq. 3 and Eq. 4 describe the behaviour of active suspension systems. In contrast to passive suspension systems, these equations include an additional term, $u(t)$, which represents the force generated by the active control system. This force is introduced into the equations to account for the active control action that actively adjusts the suspension system's behaviour in response to the road input.

$$m_2\ddot{x}_2 + b(\dot{x}_2 - \dot{x}_1) + k_2(x_2 - x_1) = u \tag{5}$$

$$m_1\ddot{x}_1 + b(\dot{x}_1 - \dot{x}_2) + k_2(x_1 - x_2) + k_1(x_1 - x_0) = -u \tag{6}$$

Eq. 5 and Eq. 6 represent the equations of an ideal semi-active suspension system. In contrast to both passive and active suspension systems, in a semi-active suspension system, it is assumed that the damping coefficient of the suspension, $b(t)$, can be varied as desired over time. This allows for the adjustment of the suspension damping characteristics based on the specific requirements or conditions, providing more flexibility and adaptability compared to passive or active suspension systems.

Table 1 Nominal parameter values for passive suspension system

Parameter	Symbol	Nominal Value	Unit
Quarter mass of the car body	m_2	288.9	kg
Mass of the wheel	m_1	28.58	kg
The damping coefficient of the suspension system	b_2	850	N s m^{-1}
The coefficient of the suspension spring	k_2	10000	N m^{-1}
The coefficient of the wheel spring	k_1	155900	N m^{-1}

The nominal parameters, which are typical for passenger cars, for the model used in this study and obtained from reference, are presented in Tab. 1 [14].

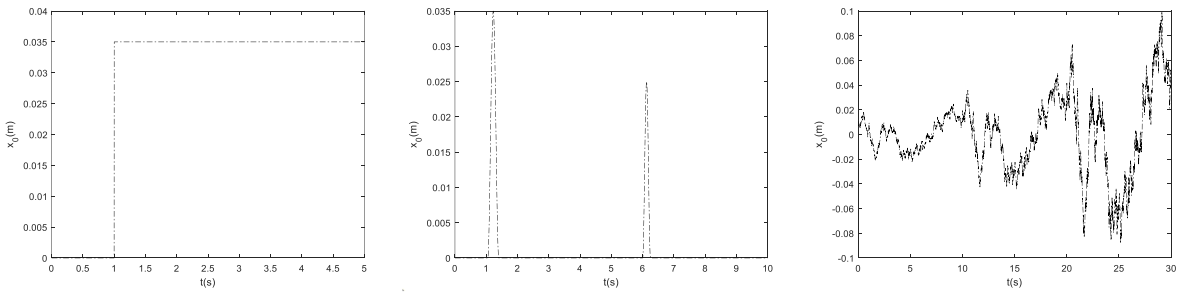

(a) (b) (c)

Fig. 2 Types of road inputs (a) Step (b) Double bump (c) ISO 8608

To ensure the thoroughness of the study, three different types of road inputs were chosen. The first type was a step input where the vehicle experienced a 0.05m step in the first second, and the movement continued at this step level. The second type was a dual bump input, in which

the controller was tested under sudden pulses, such as bumps. A test was conducted in which a sudden impact of 0.035 m was applied, followed by another impact of 0.025 m approximately five seconds later. The third and final type of road input consisted of three road inputs with varying quality levels according to ISO 8608 standards that are commonly encountered in everyday life, labelled as A-B, B-C, and C-D quality. A-B road quality represented typical roads encountered in daily life, often referred to as highways, while B-C and C-D quality roads represented more challenging conditions [15].

$$G_d(n) = G_d(n_0) * \left(\frac{n}{n_0}\right)^{-w} \tag{7}$$

Where G_d is displacement PSD (Power Spectral Density) in m^3, n is the spatial frequency, n_0 is the reference spatial frequency, which is typically defined as 0.1 cycles/m in ISO 8608 and w is the exponent of the fitted PSD.

To enhance the comprehensiveness of the study, distinct quality paths were designated within specific time ranges. The time range of $0 \leq t \leq 10$ was assigned as the "A quality path," the range of $10 \leq t \leq 20$ as the "B quality path," and the range of $20 \leq t \leq 30$ as the "C quality path." This categorization allows for a comprehensive examination and analysis of road input variations across different quality paths, enabling a more thorough investigation of the effects on the studied parameters or phenomena [16].

3 Control Algorithm

The Proportional-Integral-Derivative (PID) controller is a fundamental tool extensively employed for achieving precision regulation in industrial control systems. This controller continuously calculates the disparity between a reference point and a measured process variable, effecting corrections through the application of proportional, integral, and derivative terms.

The PID controller is represented by the following equation

$$u_{PID}(t) = K_p\left(e(t) + \frac{1}{\tau_i}\int_0^t e(t)d(t) + \tau_d\frac{de(t)}{dt}\right) \tag{8}$$

Where, $e(t) = x_{ref} - x_2$ is error ($x_{ref} = 0$), the proportional coefficient (K_p) modulates the control output in proportion to the instantaneous error, the integral coefficient (τ_i) rectifies steady-state error by integrating past errors, and the derivative coefficient (τ_d) enhances stability by anticipating future errors. There are many different methods to find these coefficients. Various methodologies, ranging from heuristic trial-and-error to more sophisticated model-based optimization techniques, facilitate the fine-tuning process. The Ziegler-Nichols method, a classic heuristic approach, offers a systematic procedure for initial coefficient estimation, paving the way for subsequent refinements.

Similar to the PID controller, the skyhook control algorithm stands as a prominent and highly efficacious control methodology within the realm of semi-active control techniques. The underlying principle of this controller, while operating straightforwardly, is elucidated in Eq. 9 for the quarter vehicle configuration.

$$\begin{cases} b(t) = b_2 & , \quad if \ \dot{x}_2(\dot{x}_2 - \dot{x}_1) \geq 0 \\ b(t) = 0 & , \quad if \ \dot{x}_2(\dot{x}_2 - \dot{x}_1) < 0 \end{cases} \tag{9}$$

In this study, this situation is simulated by only the active controller, as if there is both a semi-active control element and an active suspension element. Thus, the positive features of the two controllers were obtained. In such a case, the controller should produce the effect of both

the PID controller and the skyhook together. In this case, while for $\dot{x}_2(\dot{x}_2 - \dot{x}_1) \geq 0$ there is no value for skyhook to maximize the damping effect as in skyhook, the $b_2(\dot{x}_2 - \dot{x}_1)$ value should be added to the $u_{PID}(t)$ value to reset the damping element for $\dot{x}_2(\dot{x}_2 - \dot{x}_1) < 0$.

If there were physically both an active controller and a semi-active controller in the system, the mathematical equations would be as in Eq. 10 and Eq. 11.

$$m_2\ddot{x}_2 + b(t)(\dot{x}_2 - \dot{x}_1) + k_2(x_2 - x_1) = u_{PID}(t) \quad (10)$$

$$m_1\ddot{x}_1 + b(t)(\dot{x}_1 - \dot{x}_2) + k_2(x_1 - x_2) + k_1(x_1 - x_0) = -u_{PID}(t) \quad (11)$$

If you want to create the effect here only by combining the effect of the active controller and the semi-active element, this equation system can be done by modifying the u signal of the active system given in Eq. 3 and Eq. 4. If the modified signal is called $u_{PIDcSky}(t)$ and it is desired to obtain it from Eq. 3 and Eq. 4 with Eq. 10 and Eq. 11, if each equation is subtracted side by side,

$$b_2(\dot{x}_2 - \dot{x}_1) - b(t)(\dot{x}_2 - \dot{x}_1) = u_{PIDcSky}(t) - u_{PID}(t) \quad (12)$$

If $u_{PIDcSky}(t)$) is drawn from Eq. 12,

$$u_{PIDcSky}(t) = u_{PID}(t) + b_2(\dot{x}_2 - \dot{x}_1) - b(t)(\dot{x}_2 - \dot{x}_1) \quad (13)$$

Skyhook control algorithm is given in Eq. 9. Since $b(t) = b_2$ when $\dot{x}_2(\dot{x}_2 - \dot{x}_1) \geq 0$, $b(t) = 0$ when $\dot{x}_2(\dot{x}_2 - \dot{x}_1) < 0$, these values are written in Eq.13,

$$u_{PIDcSky}(t) = \begin{cases} u_{PID}(t) & , \quad if \ \dot{x}_2(\dot{x}_2 - \dot{x}_1) \geq 0 \\ u_{PID}(t) + b_2(\dot{x}_2 - \dot{x}_1) & , \quad if \ \dot{x}_2(\dot{x}_2 - \dot{x}_1) < 0 \end{cases} \quad (14)$$

is obtained.

While its conceptual simplicity may belie its true potential, this innovative active control methodology has demonstrated remarkable efficacy in the results section. It is appropriate to call this method “PID combined skyhook, (PIDcSky)” by its nature.

While it is true that obtaining PID coefficients through various optimization techniques could potentially yield improved outcomes, to emphasize the operational principle of the algorithm and demonstrate its efficacy, the classical Ziegler-Nichols method was employed ($K_p = 75000$, $\tau_i = 0.14$, $\tau_d = 0.035$). The coefficients thus derived for the classical PID configuration were subsequently directly applied to PID Combined Skyhook (PIDcSky). This deliberate choice allowed for the illustration of the algorithm's noteworthy performance even in the absence of optimization efforts, thereby highlighting the inherent proficiency of the control methodology.

4 Numerical Results

The behaviour of the vehicle according to the step road entrance is given in Fig. 3 As can be seen from the graphs, the proposed controller (PIDcSky) is far superior to the PID controller in terms of both settling time to reference value and initial peak.

Fig. 4 illustrates the acceleration graph. Notably, in the PID controller, the initial acceleration value is significantly higher. However, owing to the inherent characteristics of the skyhook, the PIDcSky controller exhibits instantaneous pulses. This phenomenon arises from the on-off structure inherent in the skyhook mechanism. It is worth noting that addressing this issue could be a focus for future studies through the implementation of an adaptive structure. Nonetheless, it is essential to clarify that, in the scope of the present study, which primarily aimed to elucidate the PIDcSky controller, an exhaustive investigation into this specific issue was not undertaken.

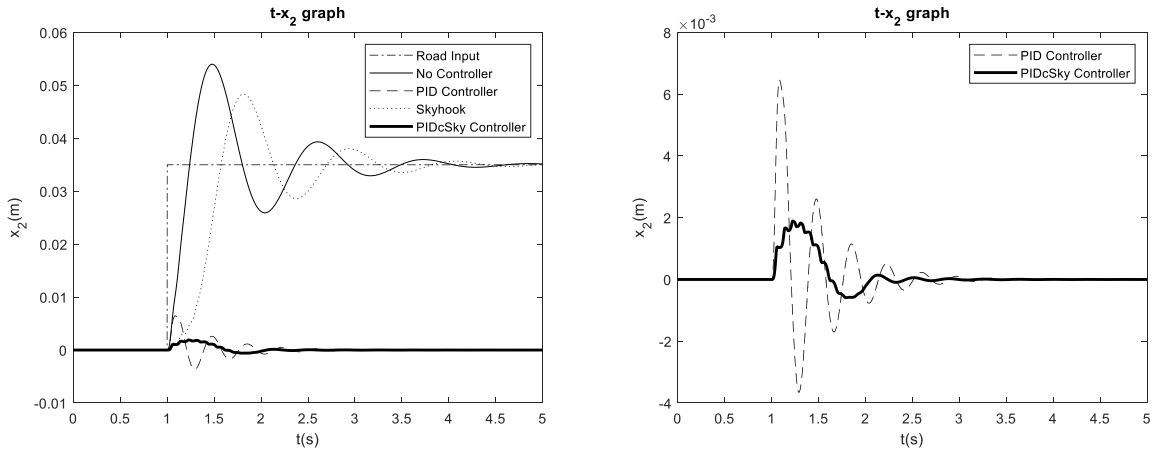

Fig. 3 For step road input (a) $t - x_2$ graph (b) $t - x_2$ graph (only the most successful two: PID and PIDcSky)

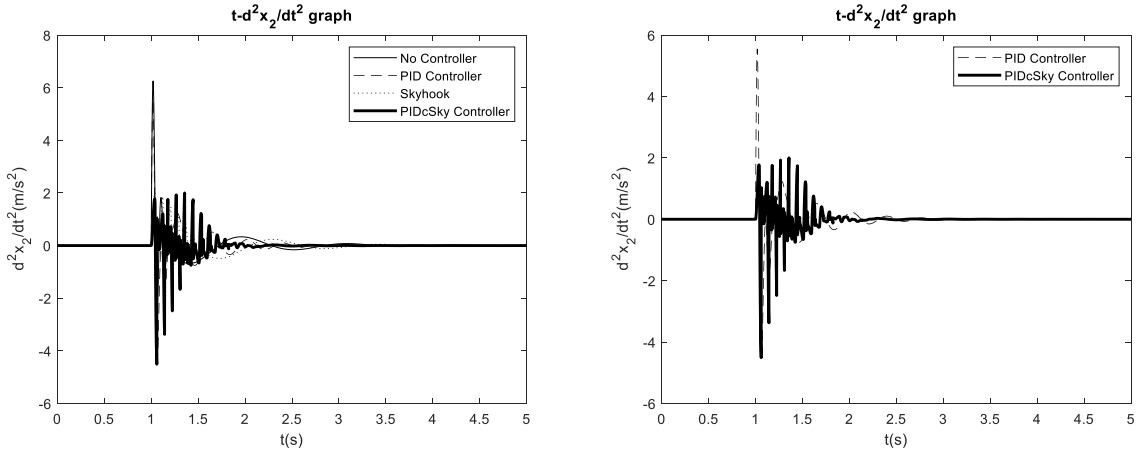

Fig. 4 For step road input (a) $t - \ddot{x}_2$ graph (b) $t - \ddot{x}_2$ graph (only the most successful two: PID and PIDcSky)

Table 2 Comparison of ISE values of Skyhook, PID, and PIDcSky controllers for step road input

	ISE(for x_2)	ISE(for $\ddot{x}_2$)
Skyhook	0.0046	1.3825
PID	$6.4822*10^{-6}$	2.9588
PIDcSky	$1.1435*10^{-6}$	1.0490

ISE values are given in Tab. 2 to evaluate the graphic representation numerically. The performance of the controller is also seen tremendously in these values.

The double bump road input is also examined to show that the performance is not just on the step road input. As can be seen in Fig. 5 and Fig. 6, the performance has increased even more at this road entrance, especially in acceleration values.

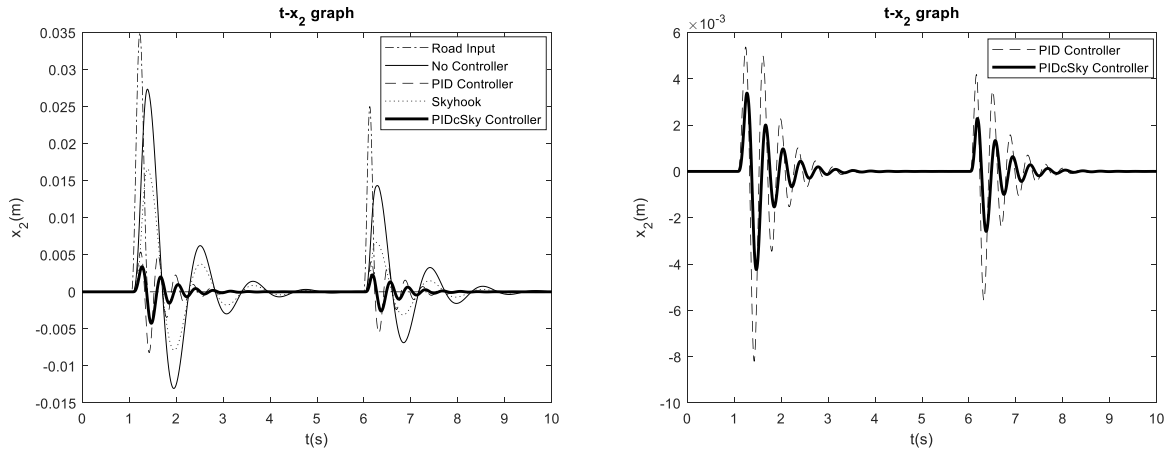

(a) (b)

Fig. 5 For double bump road input (a) $t-x_2$ graph (b) $t-x_2$ graph (only the most successful two: PID and PIDcSky)

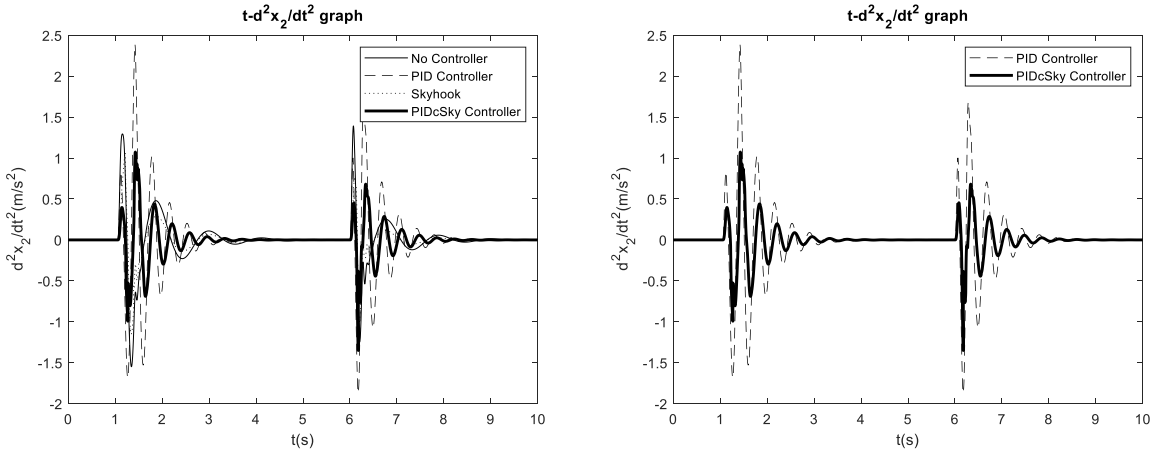

(a) (b)

Fig. 6 For double bump road input (a) $t-\ddot{x}_2$ graph (b) $t-\ddot{x}_2$ graph (only the most successful two: PID and PIDcSky)

To better express the performance of the PIDcSky controller, ISE values are given in Tab 3 comparatively.

Tab. 3 Nominal parameter values for passive suspension system

	ISE(for x_2)	ISE(for $\ddot{x}_2$)
Skyhook	$1.0566*10^{-4}$	0.6825
PID	$1.9974*10^{-5}$	3.4979
PIDcSky	$5.3738*10^{-6}$	0.7484

Finally, the behaviour of the system is examined in ISO 8608 road input, which includes various examples of all road inputs. As can be seen in Fig. 7 and Fig. 8, the PIDcSky controller is more successful than the PID controller in this road input.

To provide a more comprehensive exposition of this enhanced performance, a comparative evaluation of the ISE values is presented in Table 4. The encompassing array of road input scenarios considered encompasses a spectrum of real-world driving conditions, thereby facilitating a thoroughgoing assessment. As can be seen from the results, the proposed controller (PIDcSky) is more successful than the classical PID controller for all cases.

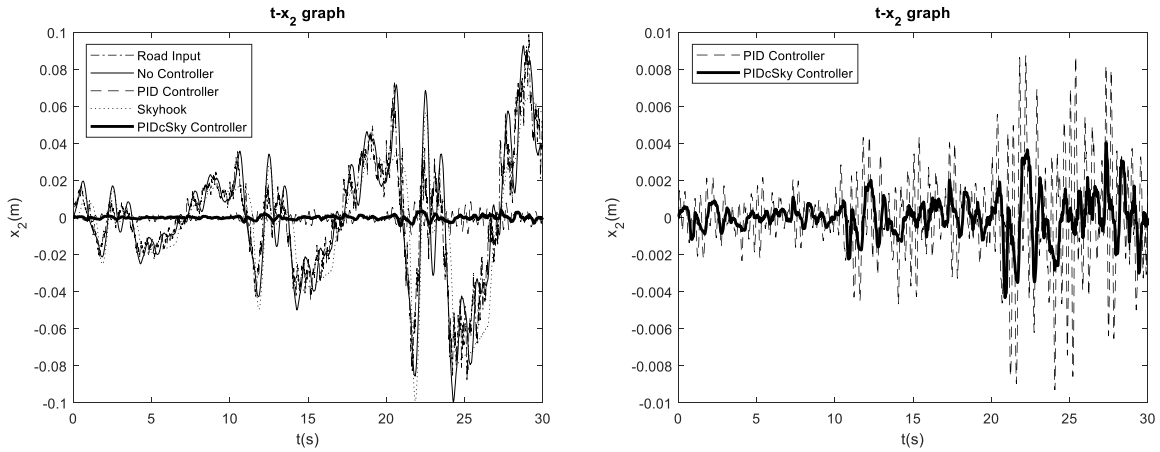

(a) (b)

Fig. 7 For ISO 8608 road input (a) $t - x_2$ graph (b) $t - x_2$ graph (only the most successful two: PID and PIDcSky)

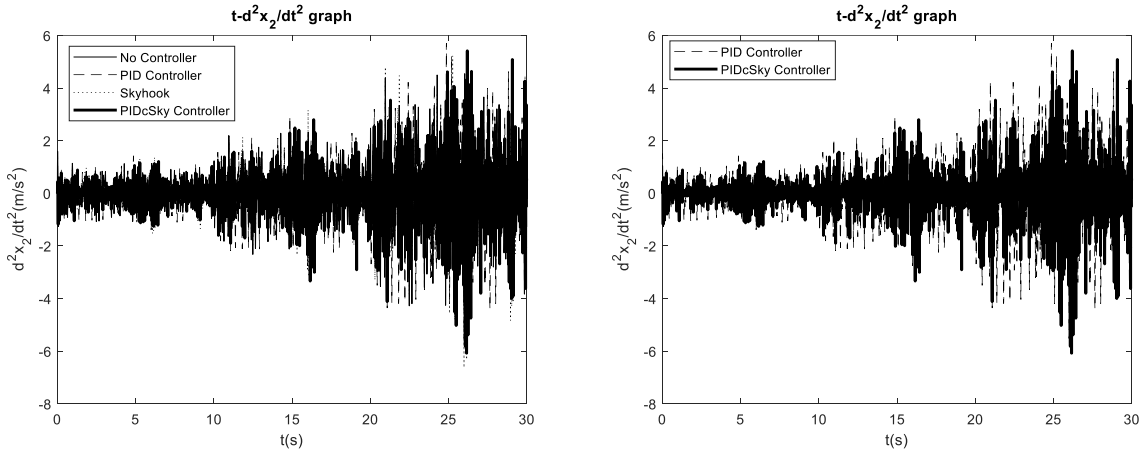

(a) (b)

Fig. 8 For ISO 8608 road input (a) $t - \ddot{x}_2$ graph (b) $t - \ddot{x}_2$ graph (only the most successful two: PID and PIDcSky)

Table 4 Comparison of ISE values of Skyhook, PID, and PIDcSky controllers for the ISO 8608 road input

	ISE(for x_2)	ISE(for $\ddot{x}_2$)
Skyhook	0.0326	41.9450
PID	$1.7144*10^{-4}$	79.7964
PIDcSky	$3.5524*10^{-5}$	28.2606

Given the impracticality of testing all possible road inputs, relying solely on time-based assessments may prove insufficient. Consequently, frequency responses were investigated, as depicted in Fig. 9. Notably, the PIDcSky controller demonstrated superior performance compared to all other controllers. It is noteworthy that the PIDcSky controller incorporates the advantageous features of both the PID controller and the Skyhook mechanism.

CONCLUSION

Skyhook employs a highly successful control algorithm as a semi-active controller, whereas PID is recognized as a classic active controller algorithm. In systems utilizing an active controller, there exists the potential for the controller to not only generate its own signal but also to simulate the signal produced by a semi-active controller. This simulation involves

considering the presence of a semi-active controller within the system. Through the integration of both signals, the system can effectively operate as if it incorporates both an active controller and a semi-active controller. This innovative approach enables the utilization of beneficial features offered by the semi-active controller alongside the characteristics of an active controller. The current study serves as a pioneering exploration, delineating a pathway for future developments in this domain.

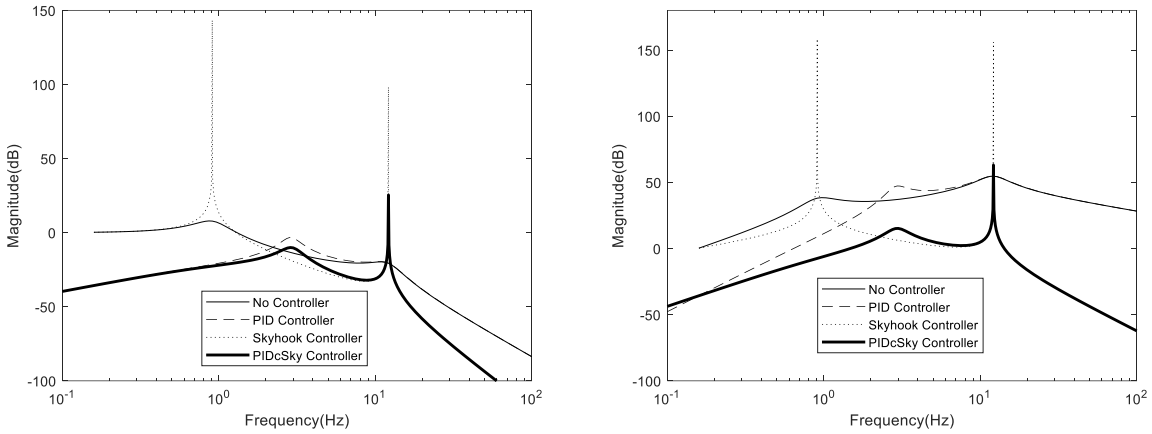

Fig. 9 Frequency response of car body (a) displacement (b) acceleration

The examination of vehicle responses to distinct road input profiles underscores the superiority of the proposed PIDcSky controller over the conventional PID controller. The analysis reveals that the PIDcSky controller outperforms its counterpart in terms of both settling time and initial peak response, as evidenced by the graphs. The effectiveness of the PIDcSky controller is further quantified through the Integral of Squared Error (ISE) values presented numerically in the previous sections, validating its performance enhancement.

Moreover, the evaluation extends beyond simple step road inputs to encompass more complex scenarios like the double bump road input. In these cases, particularly in acceleration dynamics, the PIDcSky controller demonstrates amplified efficacy, reinforcing its versatility.

The investigation also embraces ISO 8608 road inputs, incorporating a diverse array of road scenarios. the PIDcSky controller's superiority in this road input scenario, affirming its overall excellence.

In summative synthesis, the cumulative analyses underscore the ascendancy of the proposed PIDcSky controller across a wide spectrum of real-world road input scenarios. The validation attained through these varied assessments bolsters the contention that the PIDcSky controller holds significant promise in advancing suspension control under diverse conditions.

In future studies, the best parameters can be found with optimization techniques. In this study, such a path was not followed as it was compared with classical PID. In addition, many new types of controllers such as PIDcGround, and SMCcSky (Sliding Mode Control Combined Skyhook) can be produced by applying the logic of combining active and semi-active controllers in a single active controller.

REFERENCES

[1] Aström, K. J., Hägglund, T. “PID Controllers: Theory, Design, and Tuning”, 2nd ed., The Instrumentation, Systems, and Automation Society, NC, USA, **1995**. ISBN: 1-55617-516-7.

[2] Johnson, M. A., Moradi, M. H. “PID Control: New Identification and Design Methods”, Springer-Verlag London Limited, Nottingham, UK, **2005**. DOI: https: 10.1007/1-84628-148-2

[3] Ziegler, J. G., Nichols, N. B. “Optimum settings for automatic controllers”, Transactions of the ASME 64, **1942**.

[4] Xie, Y., Meng, J. “PID control for the vehicle suspension optimized by the PSO algorithm”, In: 3rd International Conference on Electromechanical Control Technology and Transportation (ICECTT 2018), Chongqing, China, pp. 172–177, **2018**.

[5] Metered, H., Abbas, W., Emam, A. “Optimized proportional integral derivative controller of vehicle active suspension system using genetic algorithm”, SAE Technical Paper, 2018-01-1399, **2018**. DOI: 10.4271/2018-01-1399

[6] Qiguo, H., Chenguang, Y. “Improved fuzzy-PID integrated control for vehicle active suspension based on road excitation”, International Journal of Vehicle Noise and Vibration 17, pp. 17 – 29, **2021**. DOI: 10.1504/IJVNV.2021.119976

[7] Karnopp, D., Crosby, M. J., Harwood, R. A. “Vibration control using semi-active force generators”, ASME Journal of Engineering for Industry 96 (2), pp. 619 – 626, **1975**. DOI: 10.1115/1.3438796

[8] Ahmadian, M., Pare, C. A. “A quarter-car experimental analysis of alternative semiactive control methods”, Journal of Intelligent Material Systems and Structures 11 (8), pp. 604 – 612, **2000**. DOI: 10.1177/1045389X0001100607

[9] Kurczyk, S., Pawełczyk, M. “Fuzzy control for semi-active vehicle suspension”, Journal of Low Frequency Noise, Vibration and Active Control 32 (3 – 4), pp. 217 – 226, **2013**. DOI: 10.1260/0263-0923.32.3-4.217

[10] Hu, G., Liu, Q., Ding, R., Li, G. “Vibration control of semi-active suspension system with magnetorheological damper based on hyperbolic tangent model”, Advances in Mechanical Engineering 9 (4), pp. 1 – 15, **2017**. DOI: 10.1177/1687814017703320

[11] Rágulík, J., Sivčák, M. “Modeling of the Controlled Air Spring”, Strojnícky časopis – Journal of Mechanical Engineering 69 (3), pp. 107 – 112, **2019**. DOI: 10.2478/scjme-2019-0037

[12] Danko, J., Milesich, T., Bucha, J. “Nonlinear Model of the Passenger Car Seat Suspension System”, Strojnícky časopis – Journal of Mechanical Engineering 67(1), pp. 23 – 28, **2017**. DOI: 10.1515/scjme-2017-0002

[13] Míša, J., Tobiáš, M., Repka, M., Straka, M., Gregor, L. “Methodology For Measuring Forces In Motorcycle Suspension Using A System Based On Analogue Potentiometers”, Strojnícky časopis – Journal of Mechanical Engineering 74 (1), pp. 91 – 102 , **2024**. DOI: 10.2478/scjme-2024-0010

[14] Leite, V. J. S., Peres, P. L. D. “Pole location control design of an active suspension system with uncertain parameters”, Vehicle System Dynamics: International Journal of Vehicle Mechanics and Mobility 43 (7), pp. 561 – 579, **2005**. DOI: 10.1080/00423110500100478

[15] ISO. “ISO 8608:2016 – Road profile”, International Organization for Standardization, Geneva, Switzerland, **2016**.

[16] Şenaslan, İ., Bilgiç, B. “Control of the quarter vehicle model with an innovative delayed resonator optimized by genetic algorithm”, Afyon Kocatepe Üniversitesi Fen ve Mühendislik Bilimleri Dergisi 24 (2), pp. 189 – 196, **2024**. DOI: 10.35414/akufemubid.1330683